

Field-theory calculation of the electric dipole moment of the neutron and paramagnetic atoms

S. A. Blundell*

SPSMS, UMR-E CEA/UJF-Grenoble 1, INAC, Grenoble, F-38054, France.

J. Griffith[†] and J. Sapirstein[‡]

Department of Physics, University of Notre Dame, Notre Dame, IN 46556

Abstract

Electric dipole moments (edms) of bound states that arise from the constituents having edms are studied with field-theoretic techniques. The systems treated are the neutron and a set of paramagnetic atoms. In the latter case it is well known that the atomic edm differs greatly from the electron edm when the internal electric fields of the atom are taken into account. In the nonrelativistic limit these fields lead to a complete suppression, but for heavy atoms large enhancement factors are present. A general bound-state field theory approach applicable to both the neutron and paramagnetic atoms is set up. It is applied first to the neutron, treating the quarks as moving freely in a confining spherical well. It is shown that the effect of internal electric fields is small in this case. The atomic problem is then revisited using field-theory techniques in place of the usual Hamiltonian methods, and the atomic enhancement factor is shown to be consistent with previous calculations. Possible application of bound-state techniques to other sources of the neutron edm is discussed.

PACS numbers: 13.40.Em, 12.39.Ba, 11.30.Er

* steven.blundell@cea.fr

† jgriffi8@nd.edu

‡ jsapirst@nd.edu

I. INTRODUCTION

One of the strongest constraints on new physics beyond the standard model is provided by measurements attempting to detect a nonvanishing electric dipole moment (edm) of the neutron, heavy atoms, or molecules [1]. This is because the extremely small value of the edm of quarks and the electron in the standard model means that any detection with presently available sensitivities arises from such new physics. According to Schiff's theorem [2], the edm of atoms or molecules arising from an electron edm vanishes in the nonrelativistic limit. However, the power of experiments on heavy atoms or molecules to put limits on a possible electron edm d_e is in fact increased by orders of magnitude because of a large violation of Schiff's theorem discovered by Sandars [3], which stems from relativistic effects. Typical values of the enhancement factor R , defined by

$$d_{\text{atom}} = R d_e, \tag{1}$$

are $R = 120$ for cesium [4] and $R = -685$ for thallium [5]. These calculations of R are carried out in a Hamiltonian formalism, with the relativistic many-body problem treated using many-body perturbation theory (MBPT), generally summing infinite classes of MBPT diagrams for higher accuracy.

One of the purposes of the present paper is to recalculate the enhancement factor for paramagnetic atoms, specifically thallium and the alkali metals lithium through francium, using a different formalism, one which treats corrections in terms of one photon exchange. Our aim here is not to achieve high accuracy in the many-body part of the problem, but rather to formulate the calculation in a field-theoretic framework [6]. This framework allows us to address the main purpose of the paper, calculating the neutron edm induced when the up and down quarks have edms d_u and d_d respectively. We are specifically concerned with the question of how the internal electric fields arising from the charged quarks affect the edm of the bound state, since their role is so important in the atomic case. In order to apply the techniques of atomic physics to the neutron, we treat the up and down quarks as moving freely in a confining well. This is a simplified version of the MIT bag model [7], without complicating issues such as bag pressure and the nonlinear boundary condition; we also neglect gluon exchange. We refer to this approach as the static well model in the following. The model is known to give the neutron (and proton) magnetic moment to within 20 percent of the experimental value when the quarks are treated as nearly massless particles

with magnetic moments coming from their confinement in the well [8], so using it to evaluate the neutron edm that arises from nonvanishing values of d_u and d_d should give results of similar accuracy.

The paper is organized as follows. In the next section we introduce the bound-state field theory tools that will be used for both the neutron and paramagnetic atom calculations, both of which are variations of the Furry representation [9]. In the following section we calculate first the lowest-order edm of the neutron, finding a 17 percent reduction from the standard nonrelativistic result, and then evaluate the effect of one photon exchange between quarks, which is equivalent to calculating the effect of the internal electric fields in the neutron. This effect will be shown to be quite small, so that despite the highly relativistic nature of the quarks within the model, we do not find large edm enhancement factors for the neutron. We then turn to the atomic problem, beginning with a brief description of the violation of Schiff's theorem [2] in atomic physics for paramagnetic atoms, after which we present a field-theoretic treatment of the problem analogous to that used for the neutron. We show that the approach leads to a suppression for light alkalis along with the well-known large enhancement factors for heavy atoms. In the concluding section we discuss how different sources of CP nonconservation could be treated with the methods described here, and also ways in which the atomic calculations could be improved.

Because we will be dealing with elementary particles with different electric charges, in the following we will present all formulas with factors of q_a , with $q_e = -e$, $q_u = 2/3e$, and $q_d = -1/3e$, e taken to be positive.

II. BOUND-STATE FIELD THEORY

For both problems treated here we assume spherical symmetry, and we expand field operators in terms of solutions to the Dirac equation

$$\psi_n(\vec{r}) = \frac{1}{r} \begin{pmatrix} ig_n(r)\chi_{\kappa\mu}(\hat{r}) \\ f_n(r)\chi_{-\kappa\mu}(\hat{r}) \end{pmatrix}, \quad (2)$$

with energy eigenvalues ϵ_n , and where $\chi_{\kappa\mu}$ is a spherical spinor. To treat the bound state problem we use variants of the Furry representation, originally introduced to evaluate QED effects in hydrogen. This representation can be thought of as intermediate between the standard interaction and the Schrödinger representations.

To transform from the Schrödinger to the interaction representation the unitary transformation

$$|\phi_I(t)\rangle = e^{iH_0 t} |\phi_S(t)\rangle \quad (3)$$

is carried out, with

$$H_0 = \int d^3x \psi^\dagger(x) [\vec{\alpha} \cdot \vec{p} + \beta m] \psi(x). \quad (4)$$

In the Furry representation, the unitary transformation is

$$|\phi_F(t)\rangle = e^{i\tilde{H}_0 t} |\phi_S(t)\rangle. \quad (5)$$

where, defining $r = |\vec{x}|$,

$$\tilde{H}_0 = \int d^3x \psi^\dagger(x) [\vec{\alpha} \cdot \vec{p} + \beta m(r) - \frac{Z\alpha}{r}] \psi(x). \quad (6)$$

We have replaced the standard electron mass term βm with a position-dependent mass for later generalization to the static well model, though it is of course constant in atomic physics. This representation is used to this day to treat radiative corrections in hydrogen and hydrogenic ions, where the primary role of the nucleus is to provide a classical Coulomb field centered at the origin, which introduces the extra term into \tilde{H}_0 . (Finite nuclear size effects, which are particularly important for highly charged ions, are accounted for by taking $Z \rightarrow Z(r)$, with $Z(r)$ modeled by a Fermi distribution).

After the transformation to the Furry representation the interaction Hamiltonian (for the atomic problem) has the usual form

$$H_I = q_e \int d^3x \bar{\psi}(x) \gamma_\mu \psi(x) A^\mu(x) \quad (7)$$

with A^μ the quantized radiation field, but with the electron field operators now expanded in terms of solutions to the Dirac equation in an external Coulomb field of the form given in Eq. (2).

To evaluate energy corrections, a generalization of the Gell-Mann–Low approach introduced by Sucher [10] can be used,

$$\Delta E = \lim_{\epsilon \rightarrow 0, \lambda \rightarrow 1} \frac{i\epsilon}{2} \frac{\partial}{\partial \lambda} \ln \langle \phi | T(e^{-i\lambda \int dx_0 e^{-\epsilon|x_0|} H_I(x_0)}) | \phi \rangle, \quad (8)$$

which has an S -matrix modified by the factor $e^{-\epsilon|x_0|}$, included in order to adiabatically turn off the interaction at large positive and negative times. This allows standard Feynman

diagram techniques to be applied, with the adiabatic factor usually leading trivially to a factor $1/\epsilon$ that cancels the ϵ in the numerator of the above formula.

In this work we are interested in treating many-electron atoms and the neutron, but only slight modifications of the approach used for hydrogen described above are needed. We start with the neutron. We model it as three light quarks confined in a spherical well of radius $R = 1.2$ fm, choosing the scalar mass of the quarks to be finite inside the well and infinite outside, which leads to the boundary conditions of the MIT bag model [7]. Just as with the description of hydrogen, we note that there is a fixed origin, in this case the center of the well instead of the position of the nucleus. In both cases this is equivalent to neglecting recoil effects. Because the masses of the up and down quarks we will be considering are very light, we set them equal to zero. The calculations presented below were tested with nonzero quark masses and found to be insensitive to this approximation. A simplification of choosing the up and down quark masses to be equal is that the spatial wave functions are then identical.

For the neutron, then, we take

$$\tilde{H}_0 = \sum_i \int d^3x [\psi_{ui}^\dagger(x) [\vec{\alpha} \cdot \vec{p} + \gamma_0 m(r)] \psi_{ui}(x) + \psi_{di}^\dagger(x) [\vec{\alpha} \cdot \vec{p} + \gamma_0 m(r)] \psi_{di}(x)] \quad (9)$$

where i is a color index. In this case the quark fields are expanded in terms of solutions of the free Dirac equation for massless particles with MIT bag model boundary conditions. The neutron wave function consists of a product of three $1s$ wave functions [8], with

$$|n_\uparrow\rangle = \frac{\epsilon_{ijk}}{2\sqrt{18}} [-2b_{ib}^\dagger b_{jc}^\dagger b_{kc}^\dagger + b_{ia}^\dagger b_{jd}^\dagger b_{kc}^\dagger + b_{ia}^\dagger b_{jc}^\dagger b_{kd}^\dagger] |0\rangle, \quad (10)$$

where we have introduced a notation in which a and b denote spin up and down states of an up quark, and c and d spin up and down states of a down quark. The color indices i, j , and k are again understood to be summed over. The ground state energy of a massless quark when $R = 1.2$ fm is 335.9 MeV, which will be denoted ϵ_g in the following: we also denote the associated wave function as $\psi_g(\vec{x})$. This defines the starting point for our treatment of the neutron edm, and calculations involving the appropriate interaction Hamiltonians can now be carried out in a systematic manner.

We now turn to the atomic case, where we will be interested in treating atoms with many electrons, in which case the original Furry representation is inadequate. To approximate the effects of screening, we introduce a local, central potential chosen to be close to the Hartree-Fock (HF) potential. Most atomic calculations based on Hamiltonian methods in fact use

the latter potential, but its nonlocality makes it unsuitable for field theory calculations. The new free Hamiltonian is

$$\tilde{H}_0 = \int d^3x \psi^\dagger(x) [\vec{\alpha} \cdot \vec{p} + \beta m - \frac{Z\alpha}{r} + U(r)] \psi(x). \quad (11)$$

Here we use a potential, which we call the core-Hartree (CH) potential, defined by

$$U_{\text{CH}}(r) = \alpha \int_0^\infty \frac{dx}{r_m(x)} \rho(x), \quad (12)$$

where $r_m(x) = \max(r, x)$ and

$$\rho(r) = \sum_a (g_a^2(r) + f_a^2(r)) \quad (13)$$

is the sum of the charge densities of all electrons in the filled core. This potential gives results close to the HF potential. To illustrate the accuracy of the potential we note that for cesium it predicts the removal energy of the valence 6s electron to be 3.267 eV, to be compared with 3.466 eV for the HF potential result. (The experimental value is 3.894 eV.) Because we have incorporated this potential into \tilde{H}_0 , the introduction of a new interaction, which acts like a counterterm,

$$H_{\text{CT}} = - \int d^3x \bar{\psi}(x) \gamma_0 \psi(x) U_{\text{CH}}(r), \quad (14)$$

is required. At the level of perturbation theory we use in this paper it plays no role.

By working with this modified Furry representation, it is possible to put atomic many-body calculations in a field-theoretic framework, with Feynman diagrams involving Coulomb photon exchange and H_{CT} having a direct correspondence with the formulas of MBPT [11]. Physics associated with transverse photon exchange and negative-energy states enters in a well-defined manner. The issue of negative-energy states, which require care to properly include in Hamiltonian formalisms, is of course correctly treated in a field-theoretical approach. This issue was emphasized in Ref. [6].

To treat the many electrons present (up to 87 for francium), we exploit the fact that all atoms considered here have one electron outside a filled core, denoted $|O_C\rangle$. Standard methods from many-body perturbation theory can then be used to treat the paramagnetic ground states as

$$|\phi\rangle = b_v^\dagger |O_C\rangle, \quad (15)$$

where v denotes a valence electron outside a closed-shell core. For example, cesium would have v being the $6s$ state, and $|0_C\rangle$ a xenon-like core, with the 54 electrons filling the $1s-5s$, $2p-5p$, and $3d-4d$ shells. The completeness of the shells allows angular momentum identities to simplify the calculations, but summations over all the core states are still needed.

III. QUARK EDM CONTRIBUTION TO d_n

We confine our attention here to the contribution of nonvanishing edms of the up and down quark to the neutron edm. A thorough discussion of other contributions to the overall edm of the neutron is given in Chapter 13 of Ref. [1]. We will present results for the lowest order contribution, $d_n^{(1)}$, and for the correction due to internal electric fields, $d_n^{(2)}$.

A general spin-1/2 particle with edm d is described by the interaction Hamiltonian

$$H_{\text{edm}} = i\frac{d}{2} \int d^3x \bar{\psi}(x) \sigma_{\mu\nu} \gamma_5 \psi(x) F^{\mu\nu}(x), \quad (16)$$

where $F^{\mu\nu}(x)$ at this point includes both classical and quantized fields. We begin by taking the electromagnetic field to be an external constant electric field pointing in the positive z direction. A neutron with edm d_n in such a field has a linear Stark effect, with the energy shift in the rest frame of the neutron when its spin is up being

$$\Delta E = -d_n E_{\text{ext}}. \quad (17)$$

To calculate the effect the edms of up and down quarks bound in a neutron have on d_n , we need to evaluate the energy shift in the same external electric field using the static well model described above, and we will then identify the coefficient of $-E_{\text{ext}}$ as the neutron edm. Because the neutron has both up and down quarks, we generalize Eq. 16 to

$$H_{I3} = -id_u E_{\text{ext}} \sum_i \int d^3x \bar{\psi}_{ui}(x) \sigma_{03} \gamma_5 \psi_{ui}(x) - id_d E_{\text{ext}} \sum_i \int d^3x \bar{\psi}_{di}(x) \sigma_{03} \gamma_5 \psi_{di}(x) \quad (18)$$

where we have replaced $F^{\mu\nu}$ with its external-field value. It is then straightforward to apply the Gell-Mann-Low formalism to calculate the energy shift and identify the lowest-order contribution as

$$d_n^{(1)} = 0.8265 \left[\frac{4}{3} d_d - \frac{1}{3} d_u \right]. \quad (19)$$

The factor 0.8265 is the integral

$$I = \int_0^R dr [g_g^2(r) + \frac{1}{3} f_g^2(r)] \quad (20)$$

for the spherical well model with massless quarks. The same kind of integral, which apart from the factor of $1/3$ is the normalization integral, is present also in the atomic edm problem for valence $s_{1/2}$ states, but it is extremely close to unity in that case, even for heavy atoms. Here, however, because the quarks are totally relativistic, the integral changes by more than 17 percent from unity. We note that in nonrelativistic quark models the factor is taken to be exactly one. This 17 percent change from the nonrelativistic limit will turn out to dominate by far the effect of the internal electric fields in the neutron.

We now turn to the evaluation of these effects, which are associated with one photon exchange. The motivation, as mentioned above, for evaluating the effect of such terms comes from the case of atomic physics. As will be shown in the next section, in heavy atoms these terms produce large enhancement factors. Because this latter enhancement is a relativistic effect, it is difficult to form an intuitive understanding of it. We note that while several explanations have been given, a recent paper [12] raises questions about their validity, and gives a quite different derivation involving Lorentz-Fitzgerald contraction. It is our view that in such situations there is no substitute for an explicit calculation of the effect.

The electromagnetic field is now split into two parts, the classical field used in the lowest-order calculation described above, and a quantized field. This leads to three additional Hamiltonians,

$$\begin{aligned}
H_{I1} &= q_u \sum_i \int d^3x \bar{\psi}_{ui}(x) \gamma_\mu \psi_{ui}(x) A^\mu(x) + q_d \sum_i \int d^3x \bar{\psi}_{di}(x) \gamma_\mu \psi_{di}(x) A^\mu(x) \\
H_{I2} &= -q_u E_{ext} \sum_i \int d^3x x_3 \bar{\psi}_{ui}(x) \gamma_0 \psi_{ui}(x) - q_d E_{ext} \sum_i \int d^3x x_3 \bar{\psi}_{di}(x) \gamma_0 \psi_{di}(x) \\
H_{I5} &= \frac{i}{2} \sum_i \int d^3x [d_u \bar{\psi}_{ui}(x) \sigma_{\alpha\beta} \gamma_5 \psi_{ui}(x) + d_d \bar{\psi}_{di}(x) \sigma_{\alpha\beta} \gamma_5 \psi_{di}(x)] F^{\alpha\beta}(x). \tag{21}
\end{aligned}$$

In the above A^μ and $F^{\mu\nu}$ are now understood to be quantized fields. The evaluation of the diagrams we consider, shown in Fig. 1, requires a treatment of the quark propagator, which when spherical symmetry is present can be written as a partial-wave expansion in terms of κ . This can be done with simple modifications of a numerical approach developed for atomic physics described in Ref. [13]. In that paper a finite basis set using piecewise polynomials was applied to solving the Dirac equation for atoms. To discretize the spectrum the atoms were taken to be in a well with radius much larger than the size of the atom, with MIT bag boundary conditions applied at that radius. A typical application for atoms generates 50

positive-energy and 50 negative-energy states for each value of κ , with the advantage that the first few positive energy-states accurately reproduce the known positive-energy bound states. All that is needed to adapt the code to the present problem is to change units and to eliminate the potential, as there is now no nucleus, and the screening from the other quarks is treated perturbatively. We emphasize that in this approach the actual excited states of the neutron play no role: we are simply evaluating Feynman diagrams in a simple bound state treatment of the neutron, using an accurate numerical method to evaluate quark propagators. This point will be returned to below when we note that in some terms the $\kappa = 1$ part of the quark propagator vanishes when negative- and positive-energy states cancel each other, an effect which would be missed if we worked with only positive-energy states.

Fig. 2 shows a part of Fig. 1(a) that involves d_u and two factors of q_d , with an energy shift we call ΔE_{a1} . We discuss its evaluation in detail to illustrate how both the neutron and the atomic calculations are carried out. The photon and quark propagators are treated as follows. The photon part of the diagrams arising from a contraction of H_{I1} and H_{I5} is

$$\langle 0|T(A_\mu(x)F_{\alpha\beta}(y))|0\rangle, \quad (22)$$

which can be obtained from the usual Feynman gauge propagator

$$\langle 0|T(A_\mu(x)A_\beta(y))|0\rangle = -ig_{\mu\beta} \int \frac{d^4k}{(2\pi)^4} \frac{e^{-ik\cdot(x-y)}}{k^2 + i\delta} \quad (23)$$

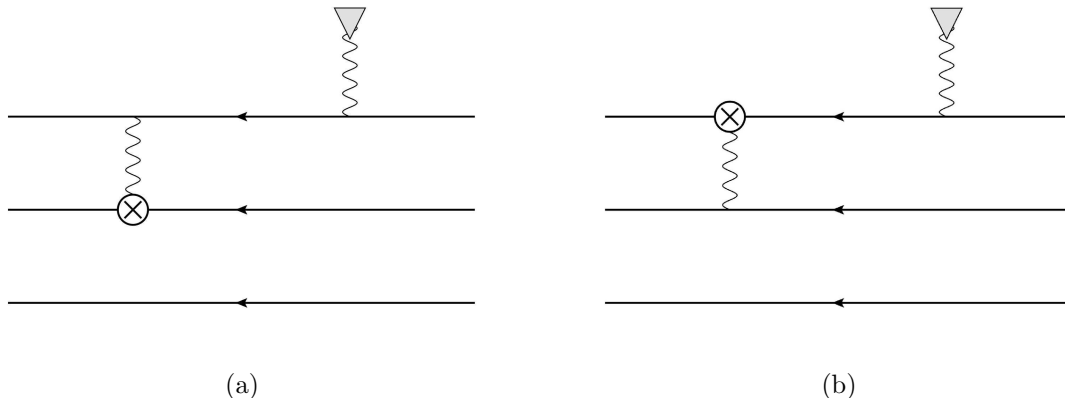


FIG. 1. The two classes of one-photon-exchange diagrams contributing to the edm of the neutron. The triangle vertex represents the external electric field, while the crossed vertex represents the edm interaction.

by differentiation. Note that the time component of the derivative operator acts on the theta functions in the time-ordering operator, but because the equal-time commutator of photon fields vanishes one has

$$\langle 0|T(A_\mu(x)F_{\alpha\beta}(y))|0\rangle = \int \frac{d^4k}{(2\pi)^4} (g_{\mu\beta}k_\alpha - g_{\mu\alpha}k_\beta) \frac{e^{-ik\cdot(x-y)}}{k^2 + i\delta}. \quad (24)$$

The quark propagator in any time-independent external field, here the static well, can be expressed as

$$\begin{aligned} \langle 0|T(\psi(x)\bar{\psi}(y))|0\rangle &= iS_F(x, y) \\ &= i \int \frac{dE}{2\pi} e^{-iE(x_0-y_0)} S_F(\vec{x}, \vec{y}; E) \\ &= i \int \frac{dE}{2\pi} e^{-iE(x_0-y_0)} \sum_m \frac{\psi_m(\vec{x})\bar{\psi}_m(\vec{y})}{E - \epsilon_m \pm i\delta} \end{aligned} \quad (25)$$

with a factor $i\delta$ for positive-energy states and $-i\delta$ for negative-energy states. The infinite sum over both positive- and negative-energy states is approximated as a finite sum using the finite basis set techniques described above.

Using these forms for the propagators Fig. 2 corresponds to the energy shift

$$\begin{aligned} \Delta E_{a1} &= -2q_d^2 d_u E_{\text{ext}} \int d^3x d^3y d^3z \int \frac{d^3k}{(2\pi)^3} \sum_m \frac{1}{\epsilon_g - \epsilon_m} \frac{e^{i\vec{k}\cdot(\vec{x}-\vec{z})}}{k^2} k_\alpha \\ &\langle n| : \psi_d^\dagger(\vec{x})\gamma_0\gamma_\beta\psi_m(\vec{x})\psi_m^\dagger(\vec{y})\gamma_3\psi_d(\vec{y})\psi_u^\dagger(\vec{z})\gamma_0\sigma^{\alpha\beta}\gamma_5\psi_u(\vec{z}) : |n\rangle. \end{aligned} \quad (26)$$

At this point we make the approximation of setting $\beta = 0$, which corresponds to accounting for internal Coulomb fields only and ignoring internal magnetic fields. We note that in the atomic case, Ref. [6] did account for magnetic terms and showed they were extremely small.

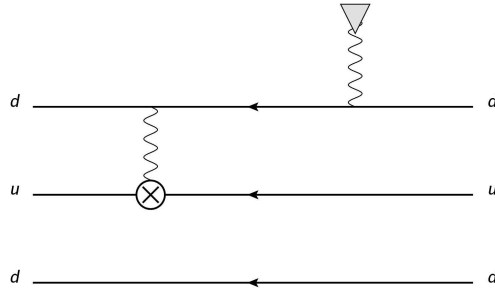


FIG. 2. Diagram 1(a) for a particular assignment of quark flavors.

For the neutron we will find very small results for the Coulomb term, and while in this more relativistic case the magnetic terms may not be as suppressed as they are in a heavy atom, they should also be very small. The integral over d^3k then can be written as a gradient of the standard integral that gives $1/|\vec{x} - \vec{z}|$. This was dealt with in two ways. In the first, a partial integration was carried out, which gives

$$\Delta E_{a1} = \frac{2q_d^2 d_u E_{\text{ext}}}{4\pi} \int \frac{d^3x d^3y d^3z}{|\vec{x} - \vec{z}|} \sum_m \frac{1}{\epsilon_g - \epsilon_m} \langle n | : \psi_d^\dagger(\vec{x}) \psi_m(\vec{x}) \psi_m^\dagger(\vec{y}) y_3 \psi_d(\vec{y}) \vec{\nabla}_z \cdot (\psi_u^\dagger(\vec{z}) \gamma_0 \vec{\Sigma} \psi_u(\vec{z})) : | n \rangle. \quad (27)$$

A useful identity for evaluating the divergence term is

$$\vec{\nabla} \cdot \bar{\psi}_m(\vec{x}) \vec{\Sigma} \psi_n(\vec{x}) = \frac{1}{x^2} \sum_{JM} I_{JM}(-\kappa_n m_n, \kappa_m m_m) Y_{JM}(\hat{x}) S_{mn}(x), \quad (28)$$

with

$$S_{mn}(x) = -(g_m(x)g_n(x))' + (f_m(x)f_n(x))' - \frac{\kappa_m + \kappa_n}{x} (g_m(x)g_n(x) + f_m(x)f_n(x)) \quad (29)$$

and

$$I_{JM}(\kappa_i \mu_i, \kappa_j \mu_j) = \int d\Omega Y_{JM}(\Omega) \chi^\dagger(\kappa_i \mu_i) \chi(\kappa_j \mu_j). \quad (30)$$

The second evaluation did not use the partial integration, but applied the gradient operator directly to the $1/|\vec{x} - \vec{z}|$ term. These two approaches gave the same numerical final result, but it should be noted that in general care is needed with partial integration in the static well model.

In evaluating the diagram, one encounters a sum over all possible magnetic quantum numbers of quarks in the initial and final neutron states, along with those of the intermediate quark propagator (which in fact can only have $\kappa = 1, -2$ from selection rules). In the atomic case, these magnetic-substate sums are always complete since we sum over the filled shells of the core, and standard identities of Racah algebra involving products of $3j$ symbols can be used to reduce the angular portion of the calculation. Because three quarks in a neutron do not form filled shells, the sums in this case are not complete and such identities cannot be immediately applied. We therefore adopted two approaches. The first simply evaluates and sums the products of the three $3j$ symbols that enter for the various combinations of magnetic quantum numbers—a ‘brute-force’ approach. In the second, which will be described in detail elsewhere, the neutron wave function (10) was rewritten in terms of

Clebsch-Gordan coefficients and a fractional parentage decomposition for the spin couplings of the quarks, after which the standard identities of Racah algebra could be applied after all. Once again, we obtained complete agreement between the two different approaches.

Now defining

$$R_{ij}(x) = g_i(x)g_j(x) + f_i(x)f_j(x), \quad (31)$$

and

$$r_{ij} = \int_0^R dx x R_{ij}(x), \quad (32)$$

the diagram of Fig. 2 gives

$$\begin{aligned} \Delta E_{a1} = & \frac{2}{243} \alpha d_u E_{ext} \sum_{n_m}^{\kappa_m=1} \frac{r_{mg}}{\epsilon_g - \epsilon_m} \int_0^R dx \int_0^R dz \frac{r_{\leq}}{r_{>}^2} R_{gm}(x) S_{gg}(z) \\ & + \frac{8}{729} \alpha d_u E_{ext} \sum_{n_m}^{\kappa_m=-2} \frac{r_{mg}}{\epsilon_g - \epsilon_m} \int_0^R dx \int_0^R dz \frac{r_{\leq}}{r_{>}^2} R_{gm}(x) S_{gg}(z), \end{aligned} \quad (33)$$

which leads to

$$d_n^{(2)}(a1) = 1.50 \times 10^{-4} d_u. \quad (34)$$

An interesting feature of the $\kappa = 1$ part of ΔE_{1a} is that it vanishes, so the result above comes entirely from the $\kappa = -2$ term. If only positive energy states are considered, a result on the order of the $\kappa = -2$ term is found, but when negative energy states are included an exact cancellation takes place. The vanishing of the $\kappa = 1$ term can be demonstrated analytically [14]. Were we to instead treat the calculation by saturating the sum with actual excited neutron p-states we would again obtain a nonzero result. The negative energy states doing the cancellation of course involve the quark sea, here treated perturbatively.

Similar manipulations apply to the other combinations of quark lines in Fig. 1, and the final formulas are, keeping only those $\kappa = 1$ terms that are nonzero,

$$\Delta E_a = -\frac{8}{729} \alpha (10d_d - d_u) E_{ext} \sum_{n_m}^{\kappa_m=-2} \frac{r_{mg}}{\epsilon_g - \epsilon_m} \int_0^R dx \int_0^R dz \frac{r_{\leq}}{r_{>}^2} R_{gm}(x) S_{gg}(z) \quad (35)$$

and

$$\Delta E_b = -\frac{8}{81} \alpha (d_u - d_d) E_{ext} \sum_{n_m}^{\kappa_m=1} \frac{r_{gm}}{\epsilon_g - \epsilon_m} \int_0^R dx \int_0^R dz \frac{1}{r_{>}} R_{gg}(x) S_{mg}(z), \quad (36)$$

which when evaluated numerically gives our result for the effect of the internal electric fields in the neutron,

$$d_n^{(2)} = 2.51 \times 10^{-4} d_u - 1.60 \times 10^{-3} d_d. \quad (37)$$

While it is of note that the contribution from the down quarks dominates that from the up quarks by an order of magnitude, the overall contribution from internal-field effects is significantly suppressed relative to the first-order neutron edm $d_n^{(1)}$ given in Eq. (19). No effect corresponding to the dramatic violation of Schiff’s theorem in heavy atoms is found, a result which we discuss further in the conclusions.

IV. ATOMIC CALCULATIONS

Turning now to the atomic case, we first note that manipulations with second-order perturbation theory are generally made that involve replacing the electric field felt by an electron in an atom, which is comprised of a one-body term coming from the nucleus and a sum of two-body terms coming from the other electrons, with a commutator. After this is done, a cancellation with first-order perturbation theory takes place, and one is left with an effective CP-violating one-body operator, the ‘Sandars operator’ [3], given by the commutator

$$[\gamma_0 \vec{\Sigma} \cdot \vec{p}, \vec{\alpha} \cdot \vec{p}] = 2\gamma_0 \gamma_5 \vec{p}^2. \quad (38)$$

This commutator would vanish if the factor γ_0 in the first term were not present. This has the advantage both of showing that Schiff’s theorem holds in nonrelativistic systems, when γ_0 is effectively close to 1, and also of allowing one to work with only a one-body operator. We note that interesting discussions of alternative ways of deriving a CP-violating one-body operator have been given in Ref. [6], where calculations for paramagnetic atoms are presented, and more recently in Ref. [15], where the theory of the edm of diamagnetic atoms is treated in detail.

If the original Sandars form is used in a first order MBPT calculation, a useful feature of the CH potential is that the result turns out to be exactly equal to the sum of the dominant three terms of the field theory calculation to be presented below. This is a special property of the CH potential, and use of other local potentials, while still dominated by the same three terms, gives results that differ from first order MBPT. Two of the three terms have already been encountered in the neutron calculation, but for the atomic problem an electric field arising from the nucleus is now present, so that we need to include an additional interaction

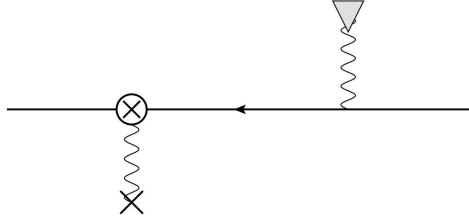


FIG. 3. A diagram representing the interaction of the valence electron's edm with the Coulomb field of the nucleus, represented by an X .

Hamiltonian,

$$H_{I4} = -id_e q_e \int d^3x \bar{\psi}(x) \sigma_{0i} \gamma_5 \psi(x) \frac{x_i}{4\pi r^2} \left[\frac{Z(r)}{r} - Z'(r) \right]. \quad (39)$$

The interaction Hamiltonians used in the neutron calculation all have atomic analogs, which can be taken from the previous section by eliminating the sums over color, dropping terms involving the down quark, and replacing q_u and d_u with q_e and d_e , respectively. We retain the convention of keeping the valence electron spin up (the core of course has zero spin), but instead of presenting the coefficient of $-E_{\text{ext}}$, we give results in terms of R as defined in Eq. (1); that is, we also pull out a factor d_e . We illustrate the calculation with the case of cesium with the CH potential, but give results for thallium and the full set of alkalis in Table I. The MBPT result for cesium with the standard form of the Sandars operator given above is an enhancement factor of 154.657. We note that this is only first-order perturbation theory, and the difference with more complete MBPT calculations mentioned in the introduction is to be expected.

The same Feynman diagrams are present as for the neutron, but in the atomic case there is a sum over core states as the valence electron interacts with the electrons in the core. Diagrams analogous to Fig. 1 in which the photon interacts between two core states do not contribute to the atomic edm, because the core has total spin zero. In general, one external line in any Feynman diagram must correspond to a valence electron for angular symmetry reasons.

The presence of the additional Hamiltonian associated with the nuclear Coulomb field (Eq. 39) requires evaluation of the diagram of Fig. 3. The diagrams of Fig. 1 are now to be thought of as having the upper line be the valence electron and the middle line one of

the core states; a sum over all possible core states is implied for that line. There is also a second set of diagrams in which the top line is a core line and the middle line is the valence state. For both sets, the roles of external core and valence states on the left-hand side of the diagram only can also be interchanged (yielding a diagram in an ‘exchange’ rather than a ‘direct’ configuration). The lower “spectator quark” line is eliminated. A complication is the fact that there can be terms with nonvanishing energy differences flowing through the photon propagator (the neutron does involve photon exchange between quarks, but all energies are identical in that case).

The calculations are quite similar to MBPT, with three exceptions. First, as mentioned above, most atomic calculations carry out a rearrangement of the Hamiltonian that builds in Schiff’s theorem as much as possible, leaving only a one-body operator (38) that vanishes in the nonrelativistic limit, and this CP-violating operator is then treated in MBPT. Here, while the interaction with the nucleus is also a one-body operator, many of our diagrams are of two-body type, so the enhancement factor arises in a different way. Second, the electron propagators contain both positive- and negative-energy states. Finally, while the sums over positive-energy states in MBPT are generally arranged in such a way as not to include both occupied core states and excited states in a single sum, in our field-theoretic approach the electron propagator includes core states along with excited states (and negative-energy states). However, as long as a complete set of diagrams is included, cancellations will occur between different diagrams that effectively enforce this restriction where appropriate. This property was checked as part of the verification of our calculation.

Because we are not building in Schiff’s theorem, an important contribution arises from lowest order, which parallels the lowest-order neutron result. Evaluating the effect of H_{I3} for an atom with a valence $s_{1/2}$ state gives the enhancement factor

$$R_0 = \int_0^\infty dr [g_v^2(r) + \frac{1}{3}f_v^2(r)], \quad (40)$$

which, as mentioned before, is very close to 1. To exhibit Schiff’s theorem for a light alkali atom then clearly requires finding terms from the nuclear and one-photon-exchange diagrams that sum to a result close to -1 .

An interesting feature of the field-theoretic approach is that one automatically generates diagrams involving radiative corrections on either the edm or external field vertex, with a representative diagram shown in Fig. 4. The presence of such terms was noted in Ref. [6].

Techniques to evaluate QED radiative corrections in the presence of perturbing potentials have been developed in Ref. [16], and these corrections were found to have at least a factor of α suppression. For that reason, we do not treat them here.

Figure 3 leads to

$$R_{\text{nuc}} = \frac{2}{3}\alpha \sum_m^{\kappa_m = -\kappa_v} \frac{d_{vm} r_{mv}}{\epsilon_v - \epsilon_m}, \quad (41)$$

with

$$d_{ij} = \int_0^\infty dr [g_i(r)g_j(r) - f_i(r)f_j(r)] \left[\frac{Z(r)}{r^2} - \frac{Z'(r)}{r} \right]. \quad (42)$$

Since no account of the electric field coming from other electrons has yet been made, a very different result from the Sandars form of 154.657 is found,

$$R_{\text{nuc}} = -80.934. \quad (43)$$

The bulk of this comes from the $6p_{1/2}$ state, -86.354 , with the next two most important contributions being from the $5p_{1/2}$ state, 7.128 , and the $7p_{1/2}$ state, -1.182 .

Next we turn to the photon-exchange diagrams. The first diagram arises from Fig. 1(b) when the upper external lines are valence states and the middle external lines are core states. In this case, the external field interacts in the usual way with the valence electron, which subsequently has its edm interact with a core electron through photon exchange. It is this term that dominates and acts to cancel the nuclear term, as will be shown below. Other, smaller terms arise from Fig. 1(b) when the external core and valence lines are interchanged in various ways, and from Fig. 1(a). All these cases intrinsically involve two-body interactions, which are not particularly complicated to deal with. As with the neutron,

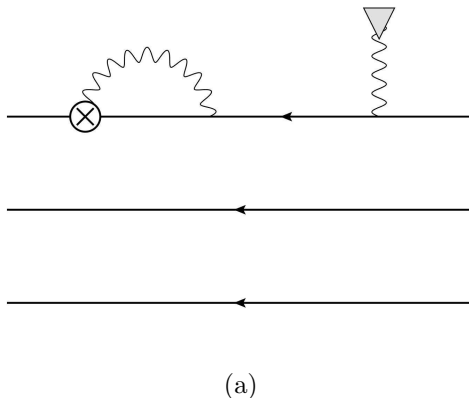


FIG. 4. Self-energy type correction to edm

we make the approximation of keeping only the $\mu = 0$ component of the photon propagator. The full expression for Fig. 1(b), including all combinations of external core and valence lines, is

$$\begin{aligned}
R_a = & -2\alpha \sum_{ma} \frac{z_{vm}}{\epsilon_v - \epsilon_m} \int \frac{d^3x d^3z}{|\vec{x} - \vec{z}|} \psi_a^\dagger(\vec{x}) \psi_a(\vec{x}) \vec{\nabla}_z \cdot (\bar{\psi}_m(\vec{z}) \vec{\Sigma} \psi_v(\vec{z})) \\
& - 2\alpha \sum_{ma} \frac{z_{am}}{\epsilon_a - \epsilon_m} \int \frac{d^3x d^3z}{|\vec{x} - \vec{z}|} \psi_v^\dagger(\vec{x}) \psi_v(\vec{x}) \vec{\nabla}_z \cdot (\bar{\psi}_m(\vec{z}) \vec{\Sigma} \psi_a(\vec{z})) \\
& + 2\alpha \sum_{ma} \frac{z_{am}}{\epsilon_a - \epsilon_m} \int \frac{d^3x d^3z}{|\vec{x} - \vec{z}|} e^{i(\epsilon_v - \epsilon_a)|\vec{x} - \vec{z}|} \psi_v^\dagger(\vec{x}) \psi_a(\vec{x}) \vec{\nabla}_z \cdot (\bar{\psi}_m(\vec{z}) \vec{\Sigma} \psi_v(\vec{z})) \\
& + 2\alpha \sum_{ma} \frac{z_{vm}}{\epsilon_v - \epsilon_m} \int \frac{d^3x d^3z}{|\vec{x} - \vec{z}|} e^{i(\epsilon_v - \epsilon_a)|\vec{x} - \vec{z}|} \psi_a^\dagger(\vec{x}) \psi_v(\vec{x}) \vec{\nabla}_z \cdot (\bar{\psi}_m(\vec{z}) \vec{\Sigma} \psi_a(\vec{z})) \quad (44)
\end{aligned}$$

where v is the valence state, the states a are core states, and the sum over m is over a complete set of states (positive- and negative-energy) arising from the intermediate electron propagator. To reach this form a partial integration has been carried out, but, as with the neutron, we also did the calculation without doing this and obtained the same result to high numerical accuracy. We have dropped two terms that do not depend on v because they vanish by angular symmetry, as mentioned earlier, which is also the case for the second term in the above expression. The dominant term is the first, which can be identified with the charge distribution of the core interacting with the edm of the valence electron; the other two terms play a much smaller numerical role.

After angular reduction, the dominant first term of R_a has the form

$$R_{a1} = \frac{2\alpha}{3} \sum_{[m][a]}^{\kappa_m = -\kappa_v} \frac{r_{vm}}{\epsilon_v - \epsilon_m} (2j_a + 1) \int_0^\infty dx \int_0^\infty dz \frac{1}{r_{>}} R_{aa}(x) S_{mv}(z). \quad (45)$$

For cesium this has the value

$$R_{a1} = 234.590, \quad (46)$$

again dominated by the $6p_{1/2}$ intermediate state, which contributes 222.327. The accumulated sum so far is now 154.657, exactly equal to the Sandars form result. We note that this pattern is quite different from Ref. [6], where the nuclear term dominates. However, the meaning of the nuclear term is different in that work, involving a factor $\gamma_0 - 1$ not present in our approach, so the disagreement is to be expected. The other terms in Eq. (44), as well as those arising from Fig. 1(a), are all much smaller (or zero), contributing to R at the level of 0.2 or less for cesium, and we will not present their values.

TABLE I. Atomic edm enhancement factors given by the present formalism using a CH potential (see text). Notation: R_0 is the lowest-order term, Eq. (40) for a valence state, R_{nuc} is the nuclear term, Eq. (41), and R_a is the dominant photon-exchange term arising from the first term in Eq. (44).

Atom	R_0	R_{nuc}	R_a	Sum
Li ($2s_{1/2}$)	1.000	-8.266	7.270	0.004
Na ($3s_{1/2}$)	1.000	-31.875	31.314	0.439
K ($4s_{1/2}$)	1.000	-66.220	68.807	3.588
Rb ($5s_{1/2}$)	1.000	-110.428	143.160	33.732
Cs ($6s_{1/2}$)	1.000	-80.934	234.590	154.657
Fr ($7s_{1/2}$)	1.000	701.730	364.161	1066.891
Tl ($6p_{1/2}$)	-0.333	-573.199	-219.132	-792.665

While of course not of interest for a practical determination of d_e , the case of lithium shows how this approach implements Schiff's theorem. The cesium results of (1, -80.934, 234.590) go to (1, -8.266, 7.270), summing to 0.004. Three features of the lithium calculation are of note. The first is that the small terms we have ignored for heavy atoms, while still summing to a small value, can be as large as 0.7 in magnitude individually. The second is that we found that the approximation of dropping the exponential terms, the no-retardation approximation, was in some cases a poor one for a particular diagram, though this had only a small effect on the total answer. The third is that using potentials other than CH fails to exhibit the almost exact cancellation shown above for lithium. In such a case presumably higher-order terms would improve the cancellation, but of course atoms that do not have a large value of R are not of interest for putting limits on d_e . In Table 1 we present the three dominant contributions to all alkali atoms and thallium along with their sums. We again emphasize that these R values correspond to first-order MBPT, and are included here to show the Schiff suppression for light atoms and the Sandars enhancement for heavy atoms, and not to represent high accuracy results.

V. CONCLUSIONS

The field-theory approach given here for calculating the edm of the neutron and paramagnetic atoms, arising from their constituents having edms, has shown firstly that for the neutron, outside of a less than 20 percent normalization shift from the nonrelativistic result, that electromagnetic corrections are small. We attribute this smallness to the fact that unlike atoms, where the energy shift associated with internal electric fields is of the order of the energy scale of atomic transitions, in the neutron the electromagnetic energy shifts are of order 1 MeV, while transition energies in the static well model are hundreds of MeV. For the neutron, the diagrams in Fig. 1 are suppressed by the ratio of the internal electromagnetic interaction energy to these excitation energies [see Eqs. (36)–(37)], giving a result three orders of magnitude smaller than the lowest-order result (19). Thus, although the quarks are highly relativistic within the model, the effect of the internal electromagnetic interactions on the edm is quite different from that found in heavy atoms, where the same class of diagrams yields large enhancement factors.

Secondly, the field-theoretic approach has provided a different way of calculating the enhancement factor R , not involving the Sandars [3] operator (38), although both one and two-body effects have to be evaluated.

We now discuss possible extensions of this approach for the case of the neutron. We note that most treatments of the neutron edm involve naive dimensional analysis, sum-rule techniques or chiral perturbation theory, as described in Ref. [1]. The approach used here, while based on a very simple static-well model, could in principle be used to provide an alternative method of calculation. A particularly interesting application could be an

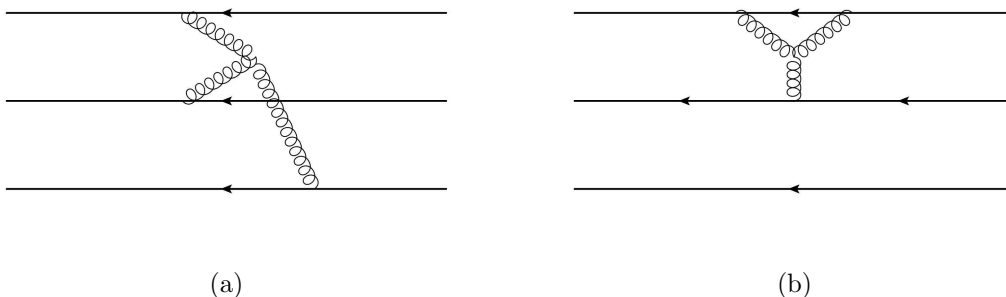


FIG. 5. Representative Weinberg 3-gluon diagrams contributing to d_n .

evaluation of the effect of Weinberg's CP-violating 3-gluon vertex [17] on d_n . This has been treated by Bigi and Uraltsev [18] and Demir, Pospelov and Ritz [19]. In the present approach one would evaluate the two diagrams shown in Fig. 5, with the understanding that the 3-gluon vertex is the source of CP-violation and that an interaction with the external electric field is to be added in all lines.

For atoms, we have demonstrated a different way of showing Schiff's theorem for nonrelativistic atoms and calculating the enhancement factor for relativistic atoms. However, the field theory here corresponds to only first-order MBPT, and it would be difficult to extend it even to second order, as ladder and crossed-ladder diagrams would have to be evaluated. The leading effect of these diagrams would be expected to reproduce second order MBPT, and arguments were given in Ref. [6] that subleading terms involving negative energy states are numerically unimportant. Probably the most interesting extension of this work in the atomic case would be to radiative corrections, but because of their smallness there seems no need at present for the considerable effort such calculations entail.

ACKNOWLEDGMENTS

The work of J.G. and J.S. was supported in part by NSF grant PHY-1068065. We thank Peter Mohr for helpful conversations.

-
- [1] *Lepton Dipole Moments*, ed. B. Lee Roberts and William J. Marciano, (World Scientific, Singapore, 2010).
 - [2] L. Schiff, Phys. Rev. **132**, 2194 (1963).
 - [3] P.G.H. Sandars, Phys. Lett. **14**, 194 (1965); Phys. Lett. **22**, 290 (1966).
 - [4] H.S. Nataraj, B.K. Sahoo, B.P. Das, and D. Memherjee, Phys. Rev. Lett. **101**, 033002 (2008); V.A. Dzuba and V.V. Flambaum, Phys. Rev. A **80**, 062509 (2009).
 - [5] Z.W. Liu and H.P. Kelly, Phys. Rev A **45**, R4210 (1992).
 - [6] A somewhat different implementation of field theory to the atomic case was previously given by E. Lindroth, B.W. Lynn, and P.G.H. Sandars, J. Phys. B **22**, 559 (1989).
 - [7] A. Chodos, R.L. Jaffe, K. Johnson, C.B. Thorn, and V.F. Weisskopf, Phys. Rev. D **9**, 3471

- (1974).
- [8] See chapter 20 of *Particle Physics and Introduction to Field Theory*, T.D. Lee, (Harwood Academic Publishers, London, 1988).
 - [9] W. Furry, Phys. Rev. **81**, 115 (1951).
 - [10] J. Sucher, Phys. Rev. **107**, 1448 (1957).
 - [11] J. Sapirstein, Rev. Mod. Phys. **70**, 55 (1998).
 - [12] E.D. Commins, J.D. Jackson, and D.P. DeMille, Am. J. Phys. **75**, 532 (2007).
 - [13] J. Sapirstein and W.R. Johnson, Phys. Lett. B29, 5213 (1996).
 - [14] P.J. Mohr, private communication.
 - [15] C.-P. Liu, M.J. Ramsey-Musolf, W.C. Haxton, R.G.E. Timmermans, and E.L. Dieperink, Phys. Rev. C **76**, 035503 (2007).
 - [16] S.A. Blundell, K.T. Cheng, and J. Sapirstein, Phys. Rev. A **55**, 1857 (1997).
 - [17] S. Weinberg, Phys. Rev. Lett. **63**, 2333 (1989).
 - [18] I.I. Bigi and N.G. Uraltsev, Nucl. Phys. B**353**, 321 (1991).
 - [19] D.A. Demir, M. Pospelov and A. Ritz, Phys. Rev. D**67**, 015007 (2003).